Electrodiffusiophoresis: Particle motion in electrolytes under direct current

Citation: Rica, Rau#l A., and Martin Z. Bazant. "Electrodiffusiophoresis: Particle motion in electrolytes under direct current." Physics of Fluids 22.11 (2010) : 112109. © 2010 American Institute of Physics

As Published: http://dx.doi.org/10.1063/1.3496976

Publisher: American Institute of Physics

Persistent URL: http://hdl.handle.net/1721.1/63159

Version: Final published version: final published article, as it appeared in a journal, conference proceedings, or other formally published context

Electrodiffusiophoresis: Particle motion in electrolytes under direct current

Raúl A. Rica[1,a)] and Martin Z. Bazant[2,b)]
[1]*Department of Chemical Engineering, Massachusetts Institute of Technology, Cambridge, Massachusetts 02139, USA and Department of Applied Physics, School of Sciences, University of Granada, Granada 18071, Spain*
[2]*Department of Chemical Engineering and Mathematics, Massachusetts Institute of Technology, Cambridge, Massachusetts 02139, USA*

(Received 8 April 2010; accepted 9 September 2010; published online 5 November 2010)

Colloidal particles in electrolytes move in response to electric fields (electrophoresis) and salt concentration gradients (diffusiophoresis), and related flows also occur at fixed surfaces (electro-osmosis and diffusio-osmosis, respectively). In isolation, these electrokinetic phenomena are well understood, e.g., electrophoresis without far-field concentration gradients and diffusiophoresis without applied electric fields. When the electrolyte passes direct current, however, concentration gradients accompany the bulk electric field (concentration polarization) and the resulting particle motion, called "electrodiffusiophoresis," involves a nonlinear combination of electrophoresis and diffusiophoresis, depending on ion transference numbers and particle properties. In this work, we analyze the electrodiffusiophoresis of spherical particles in the limit of thin double layers, neglecting surface conduction ($\mathrm{Du} \ll 1$) and convection ($\mathrm{Pe} \ll 1$), considering both nonpolarizable (fixed charge) and ideally polarizable (induced-charge) surfaces. Via asymptotic approximations and numerical solutions, we develop a physical picture to guide potential applications in electrochemical cells, such as analyte focusing, electrophoretic deposition, and microfluidic mixing near membranes or electrodes. By controlling the mean salt concentration, particle size, current, and concentration gradient, significant motion of particles (or fluid) is possible toward either electrode and toward high or low concentration. © *2010 American Institute of Physics*. [doi:10.1063/1.3496976]

I. INTRODUCTION

When a charged surface is in contact with an electrolyte solution, an electric double layer (EDL) forms. In this situation, a distribution of space charge, mainly consisting of counterions coming from the electroneutral solution, will balance the surface charge. The characteristic length along which the electrostatic fields are screened by ions in solution is the Debye length λ_D, defined by

$$\lambda_D = \sqrt{\frac{\varepsilon_r \varepsilon_0 k_B T}{\Sigma_i c_0^i (z_i e)^2}}, \tag{1}$$

ε_r being the relative electric permittivity of the liquid, typically water, ε_0 the electric permittivity of vacuum, k_B is the Boltzmann constant, T is absolute temperature, c_0^i and z_i are, respectively, the number concentration and the valence of the ionic species i, and e is the electron charge. Information about the electrical state of the interface can be obtained by provoking the relative motion of the charged liquid with respect to the solid surface. The field of science dealing with such induced motion comprises the so called electrokinetic phenomena.[1] Among these, electrophoresis of colloidal particles is perhaps the best known and the most widely investigated. It consists of the motion of colloidal particles in suspension when an electric field is applied. A simple equation relating the velocity of the particle U to a dc applied field E is the Hemholtz–Smoluchowski formula

$$U = \frac{\varepsilon_r \varepsilon_0 \zeta}{\eta} E, \tag{2}$$

where η is the viscosity of the liquid and ζ is the electrokinetic or zeta potential, which is a measure of the electric potential drop over the EDL. This equation is valid provided that the Debye length is much smaller than the radius of curvature at any point of the interface, a ($a/\lambda_D \gg 1$), and the zeta potential is not very high, in comparison with $k_B T/e$.

In deriving Eq. (2) it is assumed that the particle surface charge or zeta potential is fixed, which is determined exclusively by the ionic composition of the liquid medium. Although there exist countless studies, both theoretical and experimental, on the electrokinetic phenomena of surfaces with fixed charge (or constant zeta potential), only a few experimental works devoted to polarizable surfaces can be found, mainly in the Russian literature,[2,3] during the second half of the last century. A different situation arises when the charge is not fixed but induced by the externally applied field, and the externally applied electric field interacts with its own diffuse charge induced at ideally polarizable (blocking, fixed-potential) electrodes[4] or isolated surfaces.[5] The resulting induced-charge electrokinetic phenomena have recently attained considerable interest, due to the rich physical behavior not shown by constant-charge interfaces.[6] In particular, the task of finding how to exploit *broken symmetries* to in-

a)Electronic mail: rul@ugr.es.
b)Electronic mail: bazant@mit.edu.

duce liquid flow or colloidal migration from *a priori* symmetric and stationary flow regimes has culminated in important technological developments in microfluidic pumping[7–10] and polarizable particle manipulation.[11,12] Recent microfluidic experiments have also tested the theory of induced-charge electro-osmosis in detail by direct flow visualization,[13,14] although open questions remain, especially for large applied voltages and concentrated solutions.[15]

One of the electrokinetic phenomena that has never been investigated with polarizable surfaces is diffusiophoresis, where a charged colloidal particle moves under the action of a gradient of electrolyte concentration, and the related phenomenon of diffusio-osmosis, consisting of the flow of liquid with respect to a stationary charged surface,[16] realized that a gradient of electrolyte concentration could induce motion and provided the first theory of this effect.[17] Over the past few decades, a number of theoretical and experimental advances have been made,[18,19] and diffusion-driven motion is now an active field of research,[20–23] with results available for arbitrary values of the zeta potential, Debye length, particle size, and even volume fraction of solids.

Another missing aspect in electrokinetic analyses of polarizable particles is the simultaneous consideration of a far-field gradient of electrolyte concentration (diffusiophoresis, diffusio-osmosis) and an applied background electric field (electrophoresis, electro-osmosis). The coupled phenomenon, called "electrodiffusiophoresis" (EDP), and its related one, "electrodiffusio-osmosis" (EDO), were analyzed by Ref. 24 in the context of electrophoretic deposition. Experimental studies commonly mix these effects[25,26] and, very recently,[27] EDP has been proposed as an efficient and cheap technique for DNA sequencing. Of course, for small perturbations from equilibrium at uniform concentration, the two effects can simply be added, but there are nonlinear couplings in larger concentration gradients, which have not been experimentally accessible.

The advent of microfluidics,[28] however, presently allows researchers to achieve and control large electrolyte concentration gradients, which can also be measured by means of laser interferometry.[29] For example, sharp fronts of concentration polarization can be obtained near microchannel-nanochannel junctions,[30–32] which can also propagate as concentration shocks under appropriate conditions.[33,34] Large concentration gradients also appear in electrophoretic deposition of colloidal particles on electrodes,[35] playing an essential role in the correct control of the deposit quality. Under these conditions, a straightforward combination of electrophoresis and diffusiophoresis is not possible, as the boundary conditions usually applied on these studies are not compatible. Specifically, the constant background electric field assumed in the theory of electrophoresis breaks down in the presence of a significant gradient of electrolyte concentration.

In this work we present a study of the electrokinetic response of an isolated spherical particle in an unsupported electrolyte, in the presence of both a constant gradient of salt concentration and an applied electric current, as shown in Fig. 1(a). The assumption of a constant applied current instead of a constant electric field allows boundary conditions

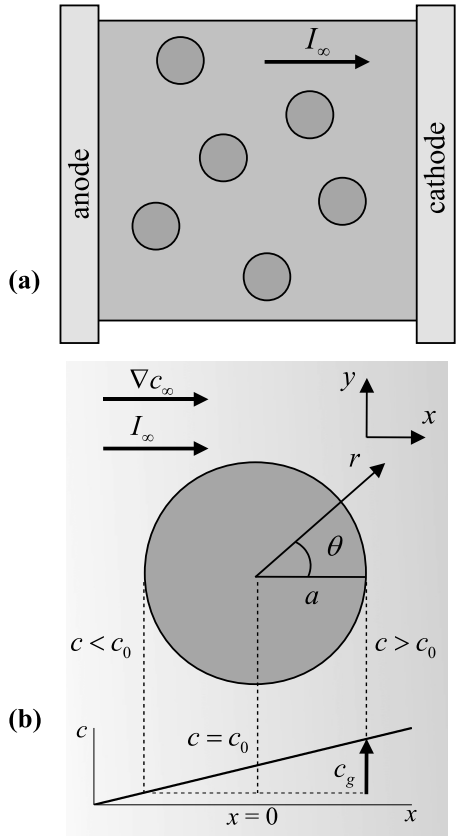

FIG. 1. Schematic picture of electrodiffusiophoresis. (a) Dispersed colloidal particles in an electrochemical cell perform phoretic motion, while fixed posts induce fluid flow, in response to a direct current between two electrodes. The former situation finds application in electrophoretic deposition or analyte focusing, while the latter could arise in electrodialysis with convection enhancing transport to ion-exchange membranes. (b) The model problem of an isolated particle or post under direct current I_∞ (taken to be positive, if it opposes diffusion) and electrolyte concentration gradient g_∞ (represented by the shading in the background). The far-field concentration profile is sketched below, with the background concentration c_0 (extrapolated at the particle center) and the gradient concentration c_g (change across one particle diameter) labeled.

on the concentration and current to be made compatible. In addition to specifying the current, we impose a concentration gradient, which can be related to the transport number $\bar{t}_+$ of (say) the cations, equal to the fraction of the current carried by those ions. Our model thus is more physically meaningful for electrochemical cells passing direct current (including microfluidic systems), since one controls the current externally and the transport number via the electrochemical selectivity of the electrodes, nanochannels, or membranes in the cell; in contrast, it is not possible to directly control the electric field and concentration gradient in the vicinity of a bulk colloidal particle (or microfluidic post). We consider both ideally polarizable and fixed charge surfaces, with the former exhibiting richer behavior, generalizing field-driven induced-charge electrokinetics in homogeneous solutions. Throughout the paper, we note various possible applications of our theoretical results in colloid science and microfluidics.

Our goal is to develop a physical picture and analytical insights into various different phenomena of EDP. As such, we make four important simplifications, which are often re-

alistic, as a first approximation. (i) We consider the limit of thin double layers (i.e., screening length much less than the particle radius, $\lambda_D \ll a$) and make use of effective electro-osmotic and diffusio-osmotic slip formulae. This assumption is ubiquitous in electrokinetics and valid for many situations of interest. (ii) We assume that surface conduction can be neglected compared to bulk conduction (i.e., small Dukhin number, $\mathrm{Du}=K^\sigma/aK_b \ll 1$, where K^σ and K_b are the surface and bulk conductivities, respectively).[1] Including surface condition is nontrivial and leads to secondary flows in cases of inhomogeneous surface charge,[36] but the net effect is typically to reduce the flow, due to "short circuiting" of the tangential electric field and/or induced-charge distribution.[37] Consideration of surface conductivity on finite Dukhin number is often complicated by the fact that it may be contributions from conduction (electromigration and diffusion) by ions located beneath the electrokinetic or slip plane. Determination of this so called Stern-layer or stagnant-layer conductivity usually requires information obtained with more than one electrokinetic technique. (iii) We neglect convective transport of ions, relative to diffusion and electromigration (i.e., small Péclet number, $\mathrm{Pe} \ll 1$, defined below). This is a good approximation for most micron-sized colloidal particles, but can lead to interesting corrections to electrophoresis in larger particles and/or faster flows.[38] On the other hand, one should consider the opposite limit $\mathrm{Pe} \gg 1$ to properly describe convective mixing (dominating diffusive mixing) in electrochemical cells. For example, below we propose the use of microfluidic posts to enhance transport to electrodes or electrodialysis membranes, near a diffusion-limited a current, but our results for $\mathrm{Pe} \ll 1$ can only be seen as a first approximation to get a sense of the possible flows available for transport enhancement. (iv) Faradaic reactions at the surfaces of electrodes are not considered in our analysis either. However, this is not a limitation in microfluidic systems, as explained below. Therefore, there is an advantage in not considering Faradaic reactions, as it gives the opportunity of extracting some common insights on the theory of electrodiffusiophoresis regardless of the specific environment where it appears.

The article is organized as follows. In Sec. II, we begin by describing the model, identifying key dimensionless groups, and solving for the slip velocity profile. In Sec. III, we proceed to derive analytical results for the particle velocity (or fluid pumping velocity, for a fixed post), as asymptotic expansions in various limits of the dimensionless groups. In Sec. IV, we solve the full problem numerically, validate the analytical results, and describe diverse phenomena that can occur as the dimensionless groups are varied across realistic parameter ranges for colloids and microfluidic devices. Finally, we conclude with a summary and discussion of possible applications of the theory.

II. MODEL

A. Bulk equations

We consider the steady state of a single freely suspended spherical colloidal particle, or a fixed two-dimensional cylindrical post, located in an infinite space containing an electrolyte solution, as shown in Fig. 1(b). Electrokinetic phenomena of particle motion (EDP) or fluid motion (EDO) are driven by a uniform direct current density I_∞ passing through the electrolyte far from the particle. In the special case where each ion has the same transference number[39] (defined below) and contributes equally to the current, the salt concentration remains constant far from the particle, and only classical electrophoresis and electro-osmosis occur. In electrochemical cells, however, this situation never occurs, as one ionic species typically carries most of the direct current in steady state, e.g., if those ions are produced or consumed by Faradaic reactions at the electrodes (as in electrodeposition/dissolution), or if they selectively pass through ion-exchange membranes (as in electrodialysis). Unequal transference numbers for the ions in steady state imply the existence of a certain constant gradient, ∇c_∞, in the neutral bulk salt concentration (derived below), which can be in either direction relative to the applied current. This concentration gradient is essential to our theory, as it drives additional diffusio-osmotic flows, contributing to the net effect of EDP.

It is important to note that a concentration gradient cannot truly exist "at infinity," since this would imply negative concentrations on one side of the particle. (This is not a problem with an electric field at infinity in the case of a uniform concentration, since the electrostatic potential can have either sign.) Instead, the concentration around the particle tends toward an asymptotic linear profile after many particle diameters, which is cut off by electrodes, walls, or membranes in the macroscopic geometry, outside the domain of the present simple model. By considering an infinite system in our analysis, therefore, we are assuming that all perturbations of the potential, concentration, and fluid velocity decay sufficiently fast to justify neglecting particle-wall interactions in a realistic finite geometry. For the colloidal problem of a particle in three dimensions, this can be an accurate approximation, since flows tend to decay like $1/r^3$ for classical electrophoresis and like $1/r^2$ for induced-charge electrophoresis. For the microfluidic problem of a post in two dimensions, the flows are longer ranged, and walls must be considered for some aspects, e.g., to compute the force needed to hold the post in place while driving the flow.[5] Nevertheless, it is a reasonable first approximation, consistent with extensive prior theoretical work, for us to focus on an isolated particle in an infinite electrolyte, in order to bring out the basic physics of EDP.

We adopt the standard electrokinetic equations for our model problem. The flux of ions in a symmetric binary electrolyte ($z^+ = -z^- \equiv z$) is given by the Nernst–Planck equation

$$\mathbf{j}^\pm = -D^\pm \nabla c^\pm \mp \frac{ze}{k_B T} D^\pm c^\pm \nabla \phi + c^\pm \mathbf{u}, \tag{3}$$

where $D^\pm$ are the diffusion coefficients of ions and $c^\pm$ their concentrations, ϕ the electric potential, and $\mathbf{u}$ is the fluid velocity. The three terms on the right hand side of this expression correspond to diffusion, electromigration, and advection contributions, respectively. Outside the EDL, electroneutrality ($c^+ = c^- \equiv c$) and charge conservation in the

stationary state ($\nabla \cdot \mathbf{j}=0$; $\mathbf{j} \equiv \mathbf{j}^+ - \mathbf{j}^-$) lead to the following set of equations:

$$D_{\text{eff}} \nabla^2 c = \mathbf{u} \cdot \nabla c, \tag{4}$$

$$\frac{ze}{k_B T} \nabla \cdot (c \nabla \phi) = -\beta \nabla^2 c, \tag{5}$$

where we have defined the effective diffusivity and the relative difference of diffusivities as follows:

$$D_{\text{eff}} = \frac{2D^+ D^-}{D^+ + D^-}, \tag{6}$$

$$\beta = \frac{D^+ - D^-}{D^+ + D^-}. \tag{7}$$

The set of equations for the motion of a suspended colloidal particle (or the flow around a post) in stationary state is completed by considering Stokes equations for the fluid motion

$$\nabla \cdot \mathbf{u} = 0, \tag{8}$$

$$\eta \nabla^2 \mathbf{u} = \nabla p, \tag{9}$$

where the electroneutrality of the bulk has been taken into account in the second expression. Here, η is the fluid viscosity and p is the dynamic pressure.

Let us now define the following quantities:

$$\tilde{\nabla} = a \nabla, \quad \tilde{r} = \frac{r}{a}, \quad \tilde{\mathbf{u}} = \frac{\mathbf{u}}{U^*}, \quad \tilde{c} = \frac{c}{c_0},$$

$$\tilde{\phi} = \frac{ze\phi}{k_B T}, \quad U^* = \frac{\varepsilon_r \varepsilon_0}{\eta a}\left(\frac{k_B T}{ze}\right)^2, \quad \text{Pe} = \frac{U^* a}{D_{\text{eff}}}.$$

With these definitions, we can rewrite Eqs. (4) and (5) in dimensionless form

$$\tilde{\nabla}^2 \tilde{c} = \text{Pe}(\tilde{\mathbf{u}} \cdot \tilde{\nabla} \tilde{c}), \tag{10}$$

$$\tilde{\nabla} \cdot (\tilde{c} \tilde{\nabla} \tilde{\phi}) = -\beta \tilde{\nabla}^2 \tilde{c}. \tag{11}$$

We can now simplify them by neglecting convective transport of ions (Pe=0),

$$\tilde{\nabla}^2 \tilde{c} = 0, \tag{12}$$

$$\tilde{\nabla} \cdot (\tilde{c} \tilde{\nabla} \tilde{\phi}) = 0. \tag{13}$$

B. Boundary conditions

The boundary conditions on the potential derive from constraints on the current density, which is the primary driving force for EDP. Neglecting surface conduction and assuming zero conductivity of the particle, the normal current density must vanish on the particle in steady state, and the current density far from the particle, j_∞ is a prescribed constant

$$\hat{n} \cdot \mathbf{j}^{\pm}|_{r=a} = 0, \tag{14}$$

$$\mathbf{j} \underset{r\to\infty}{\to} j_\infty \hat{x}, \tag{15}$$

where $\hat{x}$ is the abscissas unit vector. The boundary conditions on the salt concentration enforce impermeability of the particle to normal salt flux in steady state (neglecting surface transport) and a constant concentration gradient g_∞ far from the particle,

$$\hat{n} \cdot \nabla c|_{r=a} = 0, \tag{16}$$

$$c \underset{r\to\infty}{\sim} c_0 + g_\infty x \quad (\nabla c_\infty \to g_\infty \hat{x}). \tag{17}$$

Below we will relate g_∞ to the fraction of current carried by each ion, determined by the electrochemistry of Faradaic reactions and/or membranes in the electrochemical cell far from the particle. As a result, the steady motion of the particle is controlled entirely by the electrochemical processes involved in the passage of direct current through the electrolyte.

The boundary conditions on the fluid velocity express impermeability in the normal direction,

$$\hat{n} \cdot \mathbf{u}|_{r=a} = 0, \tag{18}$$

and the effective tangential fluid slip with respect to the particle surface, just outside the double layers,

$$\mathbf{u_s} = \frac{\varepsilon_r \varepsilon_0 \zeta}{\eta} \nabla_s \phi_s - \frac{4\varepsilon_r \varepsilon_0}{\eta}\left(\frac{k_B T}{ze}\right)^2 \ln\left(\cosh \frac{ze\zeta}{4k_B T}\right) \nabla_s \ln c_s, \tag{19}$$

where subscript s refers to surface values and tangential gradients. This is an equivalent form of the Dukhin–Deryaguin slip formula for "first kind" electro-osmosis at a thin quasi-equilibrium double layer,[40,41] also derived by Ref. 18 (to be distinguished from "second kind" electro-osmotic slip for the nonequilibrium double layer at a limiting normal current).[2,42] The first term is the classical Helmholtz–Smoluchowski electro-osmotic slip velocity (2), which persists in the absence of a concentration gradient. The second term is the diffusio-osmotic (or "chemiosmotic") slip velocity, driven by a tangential concentration gradient, first derived by Deryaguin and Dukhin in the 1960s.[16,17] For fixed charge particles, the zeta potential ζ is constant, related to the prescribed surface charge density of the particle. For ideally polarizable particles, the zeta potential is angle-dependent and related to the total charge of the particle,[5,8,11,15,43] as discussed below.

Finally, the boundary condition for the fluid flow far from the particle ($\mathbf{u}_\infty$) depends on the system under consideration. If one is interested in the motion of a particle with respect to a fluid which is at rest at infinity, the calculation is easily accomplished in the case of circular cylinders and spheres using the following expression obtained from the reciprocal theorem for Stokes flows:[11,44]

$$\mathbf{U^{cyl}} = \frac{-1}{2\pi} \int_0^{2\pi} \mathbf{u_s^{cyl}}(\theta) d\theta, \tag{20}$$

$$\mathbf{U}^{\mathbf{sph}} = \frac{-1}{4\pi}\int \mathbf{u}_s^{\mathbf{sph}}(\theta,\phi)d\Omega. \tag{21}$$

By symmetry, there is no rotational motion. In the case of microfluidic systems, we consider the flow around fixed structures rather than particle motion. The problem is then solved by adding to the motion described above an equal but opposite fluid flow that holds the particle fixed upon the combination of those two flow fields. Thus

$$\mathbf{u}_\infty = -\mathbf{U}. \tag{22}$$

Below, we will refer to **U** as the electrodiffusiophoretic velocity (EDV), with the understanding that it can describe either the motion of suspended particles (typically spheres) or fluid pumping by fixed posts (typically cylinders).

C. Dimensionless slip velocity profile

Fortunately, it is possible to obtain an exact solution to the nonlinear equations for the ionic concentration, Eq. (12), and electric potential, Eq. (13), in two or three dimensions, regardless of the boundary condition on the potential across the EDL (either constant or induced zeta potential). For a cylindrical post in $d=2$ dimensions or a spherical particle in $d=3$ dimensions, the solution for Laplace equation for the bulk salt concentration is given by

$$\tilde{c}(\tilde{r},\theta) = 1 + \frac{c_g}{2c_0}\tilde{r}\cos\theta\left(1 + \frac{1}{(d-1)\tilde{r}^d}\right), \tag{23}$$

where we have defined the quantity $c_g = 2ag_\infty$. It has dimensions of a concentration and gives information of the change on the electrolyte concentration due to the gradient along a distance equal to the particle size. In all previous works considering diffusiophoresis or diffusio-osmosis, c_g has been supposed to be infinitesimal as compared to the background electrolyte concentration c_0.[18–20,23] If this assumption is relaxed, then Eq. (23) predicts negative values of the electrolyte concentration at finite distances from the particle, due to our neglect of boundaries, such as electrodes or membranes, in the model problem. Nevertheless, as long as boundary effects on the concentration, potential, and fluid velocity are weak, it is still interesting and valid to consider moderate electrolyte concentration gradients, $c_g \ll c_0$.

In steady state, the electrostatic potential is given by the diffusion potential,[39] which reflects concentration polarization (departures from Ohm's law),

$$\tilde{\phi} = -\left(\beta + \frac{c_j}{c_g}\right)\ln\left(\frac{c}{c_0}\right), \tag{24}$$

where the prefactor is obtained from the current boundary condition at infinity, Eq. (15). Due to our simple Neumann boundary conditions, this algebraic relation between concentration and potential holds in any dimension and can be understood as a consequence of conformal invariance of the neutral Nernst–Planck equations.[45] The parameter c_j is defined by

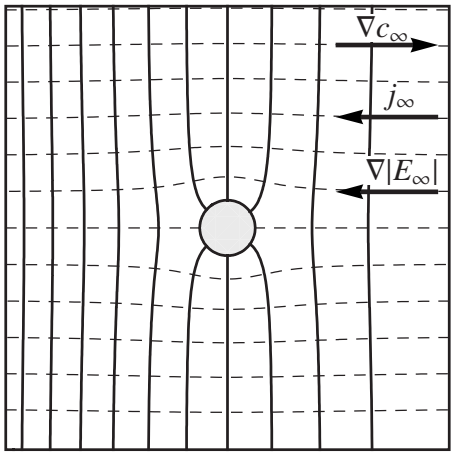

FIG. 2. Lines of constant electric potential (solid) and field lines (dashed) according to Eq. (24).

$$c_j = \frac{(1-\beta^2)aj_\infty}{D_{\mathrm{eff}}} \tag{25}$$

and has, as c_g, dimensions of concentration. This new quantity is the current density of ions scaled with the effective diffusivity and the radius of the particle. Figure 2 illustrates the structure of field and equipotential lines (out of the EDL) predicted by Eq. (24). As it can be seen, these lines correspond to those of an insulator. The peculiarity here is the depicted gradient of electric field, represented by the varying distance between equipotential lines. As we can see, the field is stronger in the low concentration region, while it is diminished where the ionic strength is higher.

Once the ionic and electric problems have been solved, we need to calculate the slip velocity on the surface of the particle, Eq. (19), in order to evaluate the integral in Eq. (20). It is convenient and instructive to cast the slip velocity in dimensionless form, taking into account the obtained results for $\tilde{c}$ and $\tilde{\phi}$, Eqs. (23) and (24), respectively. For that purpose, we define here three new dimensionless groups

$$\tilde{c}_g = \frac{c_g}{c_0}, \quad \tilde{c}_j = \frac{c_j}{c_0}, \quad \alpha = \frac{c_j}{c_g}, \tag{26}$$

which generally govern the different regimes of steady state EDP, as shown below. The first dimensionless group, $\tilde{c}_g \ll 1$, measures the strength of the concentration gradient, as the ratio of the change in far-field concentration across a distance of one particle diameter to the background concentration (extrapolated to the particle center). As noted above, this parameter cannot get close to 1, or negative concentrations will be predicted close to the particle, thus invalidating our neglect of the finite distances to the electrodes. The second dimensionless group, $\tilde{c}_j$, which can take any real value (positive, zero, or negative) measures the ionic flux, j_∞, relative to a characteristic diffusive flux $D_{\mathrm{eff}}c_0/a$ at the scale of the particle. The third dimensionless group, α, which can also take any real value, is the ratio of the contributions of electromigration (Ohm's law) and diffusion to the applied current far from the particle.

With these definitions, the dimensionless form of Eq. (19) can be expressed as

$$\tilde{\mathbf{u}}_s^{\mathbf{cyl}} = [(\alpha+\beta)\tilde{\zeta} + 4\ln\cosh(\tilde{\zeta}/4)]\frac{\tilde{c}_g \sin\theta}{1+\tilde{c}_g\cos\theta}\hat{\theta}, \tag{27}$$

$$\tilde{\mathbf{u}}_s^{\mathbf{sph}} = [(\alpha+\beta)\tilde{\zeta} + 4\ln\cosh(\tilde{\zeta}/4)]\frac{(3/4)\tilde{c}_g \sin\theta}{1+(3/4)\tilde{c}_g\cos\theta}\hat{\theta}, \tag{28}$$

for cylinders and spheres, respectively. In these expressions, $\tilde{\zeta}=(ze/k_BT)\zeta$ is the dimensionless zeta potential, scaled to the thermal voltage. We see here that α and β play similar roles in EDP. Of the two, however, α is the more important, since it can take any value set by the applied current α, while β is a constant and bounded material property of the electrolyte ($|\beta|<1$). Therefore, in most cases we restrict ourselves to electrolytes with both ions having the same diffusivity ($\beta=0$) in order to focus on the novel and nontrivial effect of varying α.

D. Transport numbers in electrochemical cells

In electrochemical cells, one always controls the current via the external circuit, but it is often difficult to impose a local concentration gradient in the vicinity of a particle or microfluidic post, as we have assumed in our model problem. In one-dimensional steady state, however, the concentration gradient (far from the particle) is unambiguously set by the electrochemical processes that sustain the applied current. This is why we view EDP as a well-defined phenomenon of electrokinetic (coupled electrophoretic and diffusiophoretic) response to direct current in an electrochemical cell.

To clarify the connection with external electrochemical processes, we introduce generalized transport numbers, defined here as the fraction of the total current carried by each ion far from the particle,

$$\bar{t}_+ = \frac{I^+}{I}, \tag{29}$$

$$\bar{t}_- = 1-\bar{t}_+ = \frac{I^-}{I}, \tag{30}$$

where $I=zej$, $I^+=zej^+$, and $I^-=-zej^-$. In the absence of a background concentration gradient, these definitions reduce to the standard definition of the "transference numbers" of each ion, t_+ and t_-, in electrochemistry;[39] these are material properties of the electrolyte, each equal to $t_\pm=1/2$, in the case that both ions have the same diffusivity ($\beta=0$). In our situation of a steady one-dimensional direct current, leading to concentration gradients, our transport numbers express the electrochemical processes sustaining the direct current far from the particle. For example, in a steady state electrodialysis cell, we have $\bar{t}_+=1$ and $\bar{t}_-=0$ for the case of an electrolyte sandwiched between two cation exchange membranes. A similar situation arises in an electrolytic cell, where only cations are active at the electrodes, e.g., for metallic ions consumed by electrodeposition at the cathode and electrodissolution of the anode[46] or for ions reduced to a neutral species at the cathode and produced by oxidation at the anode.[47]

Using Eqs. (3) and (24), we can relate the transport numbers to the dimensionless groups defined above,

$$\bar{t}_+ = \frac{1+\beta}{2}\left(1+\frac{(\beta-1)}{\alpha}\right), \tag{31}$$

$$\bar{t}_- = \frac{1-\beta}{2}\left(1+\frac{(\beta+1)}{\alpha}\right). \tag{32}$$

With these definitions, the far-field concentration gradient g_∞ can be substituted by, for example, $\bar{t}_+$,

$$\tilde{c}_g = ((1+\beta)-2\bar{t}_+)\frac{\tilde{c}_j}{1-\beta^2}. \tag{33}$$

If $\beta=0$, the case $\tilde{c}_g=0$ is equivalent to $\bar{t}_+=1/2$, i.e., if there is no gradient of electrolyte concentration, both ions contribute equally to the electric current. This situation ($\bar{t}_+=\bar{t}_-=1/2$) is also verified when $\tilde{c}_j \gg 1$. Another interesting limit corresponds to $|\tilde{c}_j|=\tilde{c}_g$. In this case, as in the examples above, all the current is carried by only one type of ion ($\tilde{c}_g=\tilde{c}_j \Rightarrow \bar{t}_+=0$, and all the current is carried by anions; $\tilde{c}_g=-\tilde{c}_j \Rightarrow \bar{t}_+=1$, and all the current is carried by cations). Again, we stress that these definitions of transport numbers apply to the nonequilibrium situation of a steady direct current, with a nonuniform concentration profile.

Although the cation transport number and applied current naturally specify the model problem for a given electrochemical cell, we prefer to solve the problem in terms of $\tilde{c}_g$, rather than $\bar{t}_+$, for mathematical convenience. This approach also allows us to clearly separate the contributions from electrophoresis and diffusiophoresis to the coupled phenomenon of EDP. Of course, translation of the results in terms of the transport number is straightforward to perform *a posteriori* by means of Eqs. (31) and (32).

III. ANALYSIS

In this section, we derive analytical approximations for the EDV by asymptotic analysis for various limits of the dimensionless groups defined above. We focus on cylindrical posts in two dimensions, since the analysis is more complicated for spheres, and presumably leads to qualitatively similar results. We divide the analysis into two parts. First, we consider posts with a constant surface charge, with a fixed value of ζ, and then we consider ideally polarizable posts, at a fixed potential, where ζ depends on the position on the surface.

A. Fixed surface charge

In this section, we derive an analytical expression for the EDP motion of particles with a constant zeta potential. The fluid flow around a fixed cylinder will be evaluated as a power expansion, the gradient on electrolyte concentration using as perturbation parameter. Although more general expressions are available for diffusiophoresis[23,48] and electrophoresis,[49] considering thick double layers, nonzero Péclet numbers, and even interactions among particles, none

of them apply for moderate values of the electrolyte gradient. This consideration justifies the inclusion of this derivation here.

1. Fixed charge electrodiffusiophoretic velocity for cylinders and spheres

Considering a fixed zeta potential on the particle surface, it is easy to integrate Eqs. (20) and (21) using Eqs. (27) and (28), respectively, to obtain the net EDV

$$\tilde{\mathbf{U}}^{\mathrm{cyl}} = [(\alpha+\beta)\tilde{\zeta} + 4\ln\cosh(\tilde{\zeta}/4)]\frac{1-\sqrt{1-\tilde{c}_g^2}}{\tilde{c}_g}\hat{x}, \tag{34}$$

$$\tilde{\mathbf{U}}^{\mathrm{sph}} = [(\alpha+\beta)\tilde{\zeta} + 4\ln\cosh(\tilde{\zeta}/4)]\frac{12\tilde{c}_g + (9\tilde{c}_g^2-16)\tanh^{-1}(3\tilde{c}_g/4)}{9\tilde{c}_g^2}\hat{x}. \tag{35}$$

These expressions predict three different contributions to the particle motion. The first addend is the purely electrophoretic one and is the only term that survives in the limit of uniform concentration $\tilde{c}_g \to 0$. The second one, which has been called "electrophoresis in absence of external electric fields,"[18,19] is due to the interplay between the difference in the diffusion coefficients of ions and the electrolyte gradient and vanishes in the absence of the latter. Finally, the third term is exclusively driven by the electrolyte gradient and represents chemiphoresis. These three terms affect the motion of the particle in different ways. While the chemiphoretic term always pushes the particle toward higher electrolyte concentrations, the direction of the electrophoretic ones depend on the sign of particle charge, the value of β, and the sign of the applied current.

Although the solutions given by Eqs. (34) and (35) are exact, the dependence on c_0 is made more clear by expanding it on powers of $\epsilon=\tilde{c}_g$ and assuming $\beta=0$,

$$U^{\mathrm{cyl}} \sim U^{\mathrm{sph}} \sim \frac{\varepsilon_r\varepsilon_0}{\eta}\left(\frac{k_BT}{ze}\right)^2\left(\frac{\tilde{\zeta}}{2D}\frac{j_\infty}{c_0} + 4\ln\cosh(\tilde{\zeta}/4)\frac{g_\infty}{c_0}\right). \tag{36}$$

Note that to first order in the limit of vanishing concentration gradient, the EDV of cylinders and spheres do coincide.

2. Fixed charge electrodiffusiophoretic flow around cylinders

Although series expansions exist for the Stokes flow around a sphere with a prescribed slip velocity,[50,51] they are cumbersome to apply to our general problem with a highly nonuniform (although axisymmetric) slip profile. It is considerably easier to solve for the two-dimensional Stokes flow around a cylinder, so we will focus on this case for analytical results in this section.

The fluid flow profiles around fixed cylinders may be written in terms of a stream function, related to the velocity field by

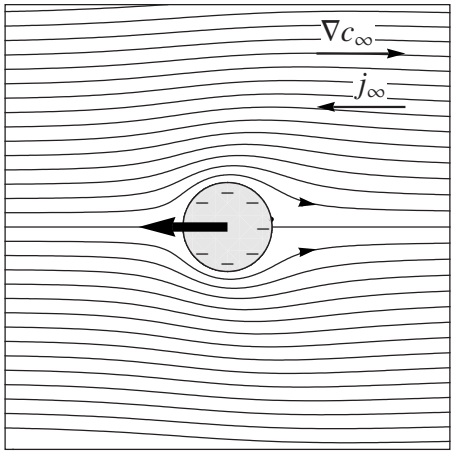

FIG. 3. Flow lines around a fixed, charged cylinder, under the action of an electrolyte concentration gradient and an electric current. Used values: $\tilde{c}_g=0.3$, $\tilde{c}_j=1$, $\tilde{\zeta}=-4$, and $\beta=0$.

$$\mathbf{u} = -\frac{\partial\psi}{\partial y}\hat{x} + \frac{\partial\psi}{\partial x}\hat{y}. \tag{37}$$

Taking the curl of the unforced Stokes equation, Eq. (9), one finds that the stream function verifies the biharmonic equation $\nabla^4\psi=0$. Exact solutions to the biharmonic equation in the plane can be expressed in Goursat form, in terms of two analytic functions of a complex variable,[45,52] but unfortunately, in this case, the problem becomes intractable due to the complicated boundary conditions, Eqs. (19) and (22).

In order to get some analytical insights, we consider the limit of small concentration gradients, via a regular perturbation expansion of the stream function in powers of $\epsilon=\tilde{c}_g$,

$$\psi = U^*(\psi_0 + \psi_1\epsilon + \psi_2\epsilon^2 + \cdots), \tag{38}$$

$$\psi_i = \sum_n A_{i,n}\left[\left(\frac{a}{r}\right)^n - \left(\frac{a}{r}\right)^{n-2}\right]\sin(n\theta). \tag{39}$$

The coefficients $A_{i,n}$ are obtained from power series expansion of the boundary conditions, Eqs. (19) and (22),

$$\mathbf{u_s} = U^*(u_{s,0} + u_{s,1}\epsilon + u_{s,2}\epsilon^2 + \cdots)\hat{\theta}, \tag{40}$$

$$\mathbf{u}_\infty = U^*(u_{\infty,0} + u_{\infty,1}\epsilon + u_{\infty,2}\epsilon^2 + \cdots)\hat{x}. \tag{41}$$

Up to $O(\epsilon^2)$, we obtain the following values for the coefficients $A_{i,n}$:

$$A_{0,1} = \tfrac{1}{2}\tilde{c}_j\tilde{\zeta},$$

$$A_{1,1} = \tfrac{1}{2}[\beta\tilde{\zeta} + 4\ln\cosh(\tilde{\zeta}/4)], \quad A_{1,2} = -\tfrac{1}{4}\tilde{c}_j\tilde{\zeta},$$

$$A_{2,1} = \tfrac{1}{8}\tilde{c}_j\tilde{\zeta}, \quad A_{2,2} = -\tfrac{1}{4}[\beta\tilde{\zeta} + 4\ln\cosh(\tilde{\zeta}/4)],$$

$$A_{2,3} = \tfrac{1}{8}\tilde{c}_j\tilde{\zeta},$$

and all other coefficients verify $A_{i,n}=0, i\leq 2$. This stream function predicts the flow pattern shown in Fig. 3, which is very similar to the well known stream lines in electro-osmosis and diffusio-osmosis around a cylinder. The slight

asymmetry in the stream lines depends almost exclusively on the magnitude of the relative electrolyte gradient, $\tilde{c}_g$.

B. Induced surface charge

1. Induced surface potential

The analysis of polarizable particles is more interesting and novel, but also more laborious. In the most general case, ζ has its origin in two contributions, each one coming from each type of charge. If the zeta potential is small ($\zeta \ll k_B T/e$), it can be expressed as the algebraic sum of those two terms,

$$\zeta = \zeta_0 + \zeta_i, \tag{42}$$

where ζ_0 is due to the pre-existing, equilibrium surface charge and ζ_i appears as a response to the action of the electric field on the (polarizable) particle. This component is angular-dependent and needs to be calculated from the values of the field-induced electric potential in the particle (ϕ_0) and the potential at the outer edge of the EDL [$\phi_s(\theta) \equiv \phi(r=a,\theta)$],

$$\zeta_i(\theta) = \phi_0 - \phi_s(\theta). \tag{43}$$

The calculation of the induced potential is based on the Gouy–Chapman theory of the EDL,[1] by computing the total surface charge

$$Q = \oint q(\zeta) dA, \tag{44}$$

where dA is the differential element of surface area and the surface charge $q(\zeta)$ is related to ζ through

$$q(\zeta) = 4(c_0 + c_g \cos\theta) z e \lambda_D \sinh\frac{ze\zeta}{2k_B T}. \tag{45}$$

In dimensionless form and 2D, we can write

$$\tilde{Q} = \tfrac{1}{2}(\exp(\tilde{\phi}_0/2)F_1 - \exp(-\tilde{\phi}_0/2)F_2), \tag{46}$$

where $\tilde{Q} = Q/4aze\lambda_D c_0$ and

$$F_1^{\mathrm{cyl}} = \int_{-\pi}^{\pi} (1 + \tilde{c}_g \cos\theta) \exp\frac{-\tilde{\phi}_s}{2} d\theta, \tag{47}$$

$$F_2^{\mathrm{cyl}} = \int_{-\pi}^{\pi} (1 + \tilde{c}_g \cos\theta) \exp\frac{\tilde{\phi}_s}{2} d\theta, \tag{48}$$

$$F_1^{\mathrm{sph}} = 2\pi \int_{0}^{\pi} \sin\theta (1 + \tilde{c}_g \cos\theta) \exp\frac{-\tilde{\phi}_s}{2} d\theta, \tag{49}$$

$$F_2^{\mathrm{sph}} = 2\pi \int_{0}^{\pi} \sin\theta (1 + \tilde{c}_g \cos\theta) \exp\frac{\tilde{\phi}_s}{2} d\theta. \tag{50}$$

Solving for the potential induced in the particle, we obtain

$$\tilde{\phi}_0 = \ln\frac{F_1 F_2 + 2\tilde{Q}^2 \pm 2\tilde{Q}\sqrt{\tilde{Q}^2 + F_1 F_2}}{F_1^2}. \tag{51}$$

As the fixed charge case has been already analyzed in the previous section, we consider here the case when $\tilde{Q}=0$ (that is, $\zeta=\zeta_i$), thus simplifying Eq. (51) to

$$\tilde{\phi}_0^{\mathrm{cyl}} = \ln\frac{\int_{-\pi}^{\pi}(1 + \tilde{c}_g \cos\theta)^{-(1/2)(\alpha+\beta-2)} d\theta}{\int_{-\pi}^{\pi}(1 + \tilde{c}_g \cos\theta)^{(1/2)(\alpha+\beta+2)} d\theta}, \tag{52}$$

$$\tilde{\phi}_0^{\mathrm{sph}} = \ln\frac{(4+\alpha+\beta)[(1+\tilde{c}_g)^{[2-(1/2)(\alpha+\beta)]} - (1-\tilde{c}_g)^{[2-(1/2)(\alpha+\beta)]}]}{[4-(\alpha+\beta)][(1+\tilde{c}_g)^{[2+(1/2)(\alpha+\beta)]} - (1-\tilde{c}_g)^{[2+(1/2)(\alpha+\beta)]}]}. \tag{53}$$

2. Induced-charge electrodiffusiophoretic velocity for cylinders and spheres

Neither the integrals in Eq. (52) nor those in Eqs. (20) and (21) in the case of ideally polarizable particles can be evaluated analytically. We obtain approximate expressions in the following section and compare their predictions to the numerical solution. The approximate solutions are obtained in the limiting situations $\tilde{c}_j \ll 1$ and $\tilde{c}_j \gg 1$, assuming in both cases $\tilde{c}_g \ll 1$. Although we consider such limits, we do not restrict ourselves to first order perturbations, and results up to $O(\epsilon^2)$ are shown, ϵ being the perturbation parameter on each regime.

a. Small currents $\tilde{c}_j \ll 1$. If we fix the exponents of $(1+\tilde{c}_g \cos\theta)$ in Eq. (52), and then expand the arguments in powers of $\epsilon = \tilde{c}_g$, that integral can be evaluated. Upon substitution in Eq. (43) the following equation is obtained for the induced zeta potential in a cylinder:

$$\tilde{\zeta}_i^{\mathrm{cyl}} = \tilde{c}_j \cos\theta + \left(\beta \cos\theta - \frac{1}{2}\tilde{c}_j(1/2 + \cos^2\theta) + \frac{3}{128}\tilde{c}_j^3\right)\epsilon + \left(\frac{-1}{2}\beta(1/2 + \cos^2\theta) + \frac{1}{3}\tilde{c}_j \cos^3\theta + \frac{9}{128}\beta\tilde{c}_j^2\right)\epsilon^2 + O(\epsilon^3), \tag{54}$$

where we have also used Eq. (24). In the case of spheres, the expression is exact,

$$\tilde{\zeta}_i^{\mathrm{sph}} = \ln\frac{(4+\alpha+\beta)[(1+\tilde{c}_g)^{[2-(1/2)(\alpha+\beta)]} - (1-\tilde{c}_g)^{[2-(1/2)(\alpha+\beta)]}]}{[4-(\alpha+\beta)][(1+\tilde{c}_g)^{[2+(1/2)(\alpha+\beta)]} - (1-\tilde{c}_g)^{[2+(1/2)(\alpha+\beta)]}]} - \left(1+\frac{3}{4}\tilde{c}_g\cos\theta\right). \tag{55}$$

Once the induced zeta potential is known, and using the slip velocity on the surface of the particle, Eqs. (27) and (28), the integrals in Eqs. (20) and (21) provide the following expressions for the EDV of an ideally polarizable particle in the presence of an electric current and a gradient of electrolyte concentration:

$$\tilde{U}^{\mathrm{cyl}} = -\tfrac{19}{64}\tilde{c}_j^2\epsilon - \tfrac{19}{32}\beta\tilde{c}_j\epsilon^2 + O(\epsilon^3), \tag{56}$$

$$\tilde{U}^{\mathrm{sph}} = -\tfrac{617}{3840}\tilde{c}_j^2\epsilon - \tfrac{617}{1920}\beta\tilde{c}_j\epsilon^2 + O(\epsilon^3). \tag{57}$$

In the case $\beta=0(D^+=D^-\equiv D)$ and $\tilde{c}_j \ll 1$, the leading term in this expansion is, including dimensions,

$$U^{\mathrm{cyl}} = -\frac{19}{32}\frac{\varepsilon_r\varepsilon_0}{\eta}\left(\frac{ak_BT}{zeD}\right)^2\frac{j_\infty^2 g_\infty}{c_0^3}, \tag{58}$$

$$U^{\mathrm{sph}} = -\frac{617}{1920}\frac{\varepsilon_r\varepsilon_0}{\eta}\left(\frac{ak_BT}{zeD}\right)^2\frac{j_\infty^2 g_\infty}{c_0^3}. \tag{59}$$

This expression predicts that, for low electric currents, an ideally polarizable particle will move toward lower electrolyte concentrations regardless of the direction of the electric current. It is also worth mentioning the strong dependence of the velocity with the electrolyte concentration, being larger the lower the concentration.

b. Large currents: $\tilde{c}_j \gg 1$. The large-$\tilde{c}_j$ approximation in the case of cylinders is more involved than the previous one. The starting point of this study requires, as before, an appropriate approximation to the value of the integrals in Eq. (52). For this purpose, we take advantage of the Laplace or saddle point method.[53] This method allows us to obtain accurate approximations to integrals of the form

$$\int_a^b e^{Nf(x)}dx, \tag{60}$$

where $f(x)$ is a twice differentiable function with a local maximum at $x_{\max}\in\,]a,b[$ and $N\gg 1$, by doing a Taylor expansion of $f(x)$ around $x_{\max}$. This method has corrections $O[(x-x_{\max})^3]$. Therefore, we can estimate the integrals in Eq. (52) and find

$$\tilde{\phi}_0^{\mathrm{cyl}} \simeq \ln\left(\left[\frac{(1\mp\tilde{c}_g)^{1-\alpha}}{(1\pm\tilde{c}_g)^{1+\alpha}}\right]^{1/2}\frac{\mathrm{erf}\left[\frac{\pi}{2}\sqrt{\pm\tilde{c}_j/(1-\tilde{c}_g)}\right]}{\mathrm{erf}\left[\frac{\pi}{2}\sqrt{[\pm\tilde{c}_j/(1+\tilde{c}_g)]}\right]}\right) \tag{61}$$

where the upper (lower) sign corresponds to $\tilde{c}_j>0$ ($\tilde{c}_j<0$) and erf is the error function. This result, together with the potential at the outer edge of the EDL, Eq. (24), provides the zeta potential from Eq. (43),

$$\tilde{\zeta}_i^{\mathrm{cyl}} = \tilde{c}_j\cos\theta + \left(\tfrac{1}{2}\tilde{c}_j(1-\cos^2\theta) + \beta\cos\theta \mp 1\right)\epsilon + \left(\tfrac{1}{3}\tilde{c}_j\cos^3\theta - \tfrac{1}{2}\beta\cos^2\theta\right)\epsilon^2 + O(\epsilon^3). \tag{62}$$

In this large-$\tilde{c}_j$ regime, the induced zeta potential is also large, and we can make the approximation $\ln\cosh\tilde{\zeta}/4\simeq\tilde{\zeta}_i - \ln 2$ in Eq. (27). As before, we cannot solve analytically the integrals (20) and (21) unless we perform a Taylor expansion of the slip condition in powers of $\epsilon=\tilde{c}_g$. After this expansion, the integrals provide, up to $O(\epsilon^2)$,

$$\tilde{U}^{\mathrm{cyl}} = \left(\tfrac{1}{16}\tilde{c}_j^2 \pm \tilde{c}_j\left(\tfrac{2}{3\pi}-\tfrac{1}{2}\right) - 2\ln 2\right)\epsilon + \beta\left(\tfrac{1}{8}\tilde{c}_j \pm \left(\tfrac{2}{3\pi}-\tfrac{1}{2}\right)\right)\epsilon^2 + O(\epsilon^3), \tag{63}$$

$$\tilde{U}^{\mathrm{sph}} = \tfrac{1}{320}(53\tilde{c}_j^2 - 365\tilde{c}_j)\epsilon + \tfrac{13}{160}\beta\tilde{c}_j\epsilon^2 + O(\epsilon^3), \tag{64}$$

with the same sign criteria as before. If $\beta=0$, the leading term of these expansions are

$$U^{\mathrm{cyl}} = \frac{1}{8}\frac{\varepsilon_r\varepsilon_0}{\eta}\left(\frac{ak_BT}{zeD}\right)^2\frac{j_\infty^2 g_\infty}{c_0^3}, \tag{65}$$

$$U^{\mathrm{sph}} = \frac{53}{160}\frac{\varepsilon_r\varepsilon_0}{\eta}\left(\frac{ak_BT}{zeD}\right)^2\frac{j_\infty^2 g_\infty}{c_0^3}, \tag{66}$$

which has corrections $O(\tilde{c}_g^3)$, and differ from the low-$\tilde{c}_j$ leading terms, Eqs. (58) and (59), only in the numerical factor and the sign, which is positive here. In this regime, particles move toward high electrolyte concentration, while the fluid flow is directed against the concentration gradient. Therefore, an inversion of the motion is predicted at values of the electric current $\tilde{c}_j\simeq 1$, depending on the value of the gradient $\tilde{c}_g$.

3. Induced-charge electrodiffusiophoretic flow for cylinders

As before, we focus on two-dimensional flows around cylinders to obtain analytical results, with the expectation that similar results will hold for spheres, treated numerically below. Again, we express the fluid flow in terms of a Taylor expansion of a stream function, Eqs. (38) and (39), up to $O(\tilde{c}_g^2)$. For these calculations, we also assume a symmetric electrolyte, $\beta=0$.

a. Small currents: $\tilde{c}_j \ll 1$. If the value of $\tilde{c}_j$ is low, we can define a new perturbation parameter $\epsilon'=\tilde{c}_j$ and neglect perturbation terms $O(\delta^5)$, where δ can be either ϵ or ϵ'. In this approximation, the coefficients $A_{i,n}$ are

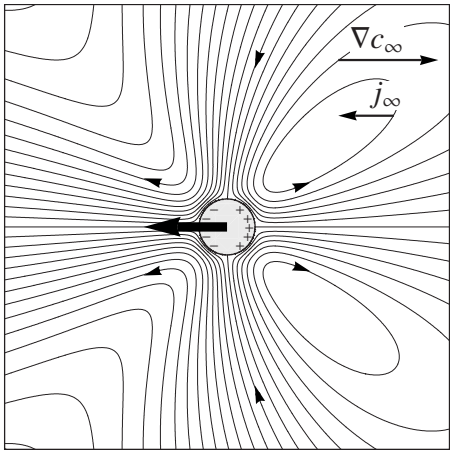

FIG. 4. Flow lines around a fixed, ideally polarizable cylinder, under the action of an electrolyte concentration gradient and an electric current in the low-c_j regime. The velocity of a moving particle points toward low electrolyte concentration. Used values: $\tilde{c}_g=0.05$, $\tilde{c}_j=0.01$, and $\beta=0$.

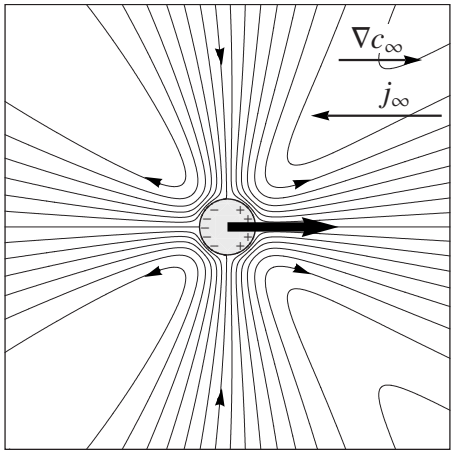

FIG. 5. Flow lines around a fixed, ideally polarizable cylinder, under the action of an electrolyte concentration gradient and an electric current in the large-c_j regime. The velocity of a moving particle points toward high electrolyte concentration. Used values: $\tilde{c}_g=0.05$, $\tilde{c}_j=100$, and $\beta=0$.

$$A_{0,2}=\tfrac{1}{4}\tilde{c}_j^2,$$

$$A_{1,1}=\frac{-1}{64}\tilde{c}_j^2\left(19-\frac{143}{192}\tilde{c}_j^2\right)$$

$$A_{1,3}=\frac{-1}{64}\tilde{c}_j^2\left(11+\frac{3}{384}\tilde{c}_j^2\right) \quad A_{2,2}=\frac{66}{192}\tilde{c}_j^2,$$

and every other $A_{i,n}=0, i\leq 2$.

Figure 4 shows an example of the flow lines obtained in this situation. As observed, the flow is a variation of the well known quadrupolar flow of an ideally polarizable particle in a uniform electric field. In that case, the perfect quadrupolar flow leads to no net motion of the fluid or the particle. The presence of a the concentration gradient breaks this symmetry, being responsible of both net fluid flow (osmosis) or motion of the particle. In this situation, a moving particle would move to the left [toward low electrolyte concentration, as predicted by Eq. (58)], while a net transport of liquid far from the particle would be directed to the right.

b. Large currents: $\tilde{c}_j^2\gg 1$. This asymptotic solution requires an extra term in the eigenvalues expansion, Eq. (39), in the form

$$\psi_i=\sum_n A_{i,n}\left[\left(\frac{a}{r}\right)^n-\left(\frac{a}{r}\right)^{n-2}\right]\sin(n\theta)$$
$$+B_i\ln\left[1+\left(\frac{a}{r}\right)^2\right]\sin\theta. \tag{67}$$

With this consideration, the obtained coefficients are

$$A_{0,2}=\tfrac{1}{4}\tilde{c}_j^2,$$

$$A_{1,1}=\frac{1}{16}\tilde{c}_j^2+\left(\frac{1}{2}-\frac{2}{3\pi}\right)\tilde{c}_j-2\ln 2,$$

$$A_{1,2}=\pm\frac{1}{4}\tilde{c}_j, \quad A_{1,3}=\frac{-3}{10}\tilde{c}_j^2, \quad B_1=\left(\frac{4}{3\pi}-2\right)\tilde{c}_j,$$

$$A_{2,2}=\tfrac{5}{48}\tilde{c}_j^2+\tfrac{1}{4}\tilde{c}_j+\ln 2, \quad A_{2,3}=\mp\tfrac{3}{16}\tilde{c}_j, \quad A_{2,4}=\tfrac{11}{96}\tilde{c}_j^2,$$

$$B_2=\pm\left(\tfrac{1}{8}\tilde{c}_j-1\right),$$

where the upper (lower) sign corresponds to $|\theta|<\pi/2$ ($|\theta|>\pi/2$) and all other $A_{i,n}$ are equal 0 if $i\leq 2$.

An example of the flows generated in this situation is depicted in Fig. 5. As is clearly seen, this flow is very similar to the one described in the low-$\tilde{c}_j$ case. As it is shown, in this case the velocity of the particle points to the right [toward high electrolyte concentration, as predicted by Eq. (65)].

IV. NUMERICAL RESULTS AND DISCUSSION

Although we have treated separately fixed charge and ideally polarizable surfaces, such a distinction is not possible in most practical situations with direct current. (In contrast, for alternating current, one can neglect the contribution of fixed charge as a first approximation.)[5,45] In general, as already stated, a polarizable surface will also possess some fixed charge, even in the absence of an applied field. Hence, before detailing the characteristic behavior of the two kinds of surfaces, it is interesting to estimate under which conditions will each type of contribution dominate. Considering that in the $\tilde{c}_j\ll 1$ regime the induced zeta potential is very low (in fact $\tilde{\zeta}_i\ll 1$) a typical value of $\zeta_0=50$ mV will suffice to make the induced-charge negligible. Hence, we will only establish the comparison in the case $\tilde{c}_j\gg 1$ by considering the leading terms of the dimensionless versions of Eqs. (36) and (66),

$$\tilde{U}_i=\tfrac{53}{320}\tilde{c}_j^2\tilde{c}_g, \tag{68}$$

$$\tilde{U}_0=\tfrac{1}{2}[\alpha\tilde{\zeta}_0+2\ln\cosh(\tilde{\zeta}_0/4)]\tilde{c}_g. \tag{69}$$

If we assume $\tilde{\zeta}_0=2$, then $2\ln\cosh(\tilde{\zeta}_0/4)\simeq 1/4$, and induced-charge effects will dominate when the parameters verify $\tilde{c}_j^2>320/53(\alpha+1/8)$. Assuming $\tilde{c}_g^2\ll 12$, the condition will be verified if $\tilde{c}_j\tilde{c}_g>6$, or more clearly

$$j_\infty g_\infty > \frac{3D}{a^2} c_0^2. \tag{70}$$

According to this, an electric current density of $I \sim 450$ mA cm^{-2} is required to make the induced-charge dominate over the fixed charge under the following conditions: $c_0=1$ mM KCl, $g_\infty=50$ mM cm^{-1}, and $a=5$ μm. This current can be lowered by increasing a or decreasing c_0, since the fixed charge contribution is independent of a and depends on c_0, while the induced-charge contribution depends on c_0^3. Note that such large currents, especially in the presence of a low background salt concentration c_0, would lead to very large electric fields, which would trigger effects we have not considered, such as surface conduction, convection, and possibly ion crowding[15] and second kind electrokinetic phenomena.[2,54] Nevertheless, it is reasonable to begin by considering the simple model of this article, based on thin quasiequilibrium double layers at moderate voltages.

The following subsection presents the main results for each particular case. Although, for simplicity, we refer mostly to colloidal particles, all our results have analogs for flows around fixed structures in microfluidic devices.

A. Fixed charge

Let us start the considerations on fixed charge surfaces coming back to Eq. (36), where two addends contribute to the motion (the first one represents the electrophoretic contribution and the second one is the chemiphoretic term). The dependence of the latter on c_0 is well known from all the previous studies on diffusiophoresis, whereas there is a substantial difference between the electrophoretic term with the Smoluchowski formula due to the presence of c_0 in the denominator. This factor has relevant implications on the behavior of both colloidal systems and microfluidic devices. For example, in the presence of a non-negligible concentration gradient, c_0 will change as the particle moves, hence modifying the local electric field responsible for the electrophoretic term. Therefore, "accelerations" of colloidal particles can be observed under the appropriate conditions of a stationary concentration gradient and constant current along the system, conditions already achieved in microfluidic experiments.[31,34,55]

In the limit of small departures from equilibrium ($\tilde{c}_g \ll 1$ and $\tilde{c}_j \ll 1$), the response of nonpolarizable, charged particles is the superposition of the well known mechanisms of electrophoresis (electro-osmosis) and diffusiophoresis (diffusio-osmosis). If these contributions act in opposite directions, the competition between them can give rise to opposite movements depending on the properties of the considered system. In fact, there is a value of the applied current at which the movement (both migration of particles and fluid flow) is reversed, given by the condition ($\mathbf{U}=0$) in Eq. (34) (note that only the first factor of the right hand side of this equation is relevant for the calculation). These considerations are similar to the well known diffusiophoresis inversion due to nonzero values of β,[56]

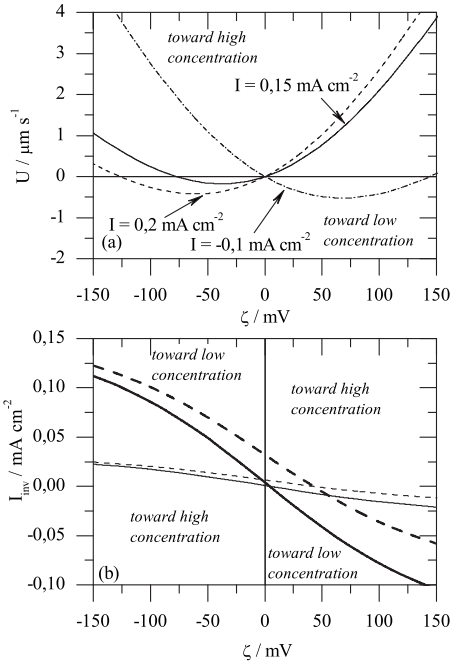

FIG. 6. (a) EDV of a charged spherical particle in the presence of an electrolyte concentration gradient ($g_\infty=50$ mM cm^{-1}) and the indicated electric current densities, as a function of the (fixed) zeta potential on the surface. Other parameters are $c_0=1$ mM KCl ($D_{\text{eff}}=2\times10^{-9}$ m^2 s^{-1}, $\beta=0$); $a=1$ μm. (b) Value of the electric current density at which the movement is reversed, I_{inv}, as a function of the zeta potential. Solid lines: KCl ($D_{\text{eff}}=2\times10^{-9}$ m^2 s^{-1}; $\beta=0$). Dashed lines: NaCl ($D_{\text{eff}}=1.6\times10^{-9}$ m^2 s^{-1}; $\beta=-0.2$). Thin lines: $g_\infty=10$ mM cm^{-1}. Thick lines: $g_\infty=50$ mM cm^{-1}.

$$I_{\text{inv}} = -\frac{2zeD_{\text{eff}}}{1-\beta^2}\left(\beta + \frac{4\ln\cosh(\tilde{\zeta}/4)}{\tilde{\zeta}}\right) g_\infty, \tag{71}$$

where all the involved quantities have been made explicit. According to this result, particles with the same type of charge on their surfaces (positive or negative) can move in opposite directions under the appropriate conditions, as it is depicted in Fig. 6(a). Note that significant opposite velocities can be reached for comparable magnitudes of the charge (for example, $\Delta U \simeq 1$ μm s^{-1} for $\zeta=-50$ mV and $\zeta=-125$ mV in the curve $I=0.15$ mA cm^{-2}). Therefore, we can define a map in the I_{inv} versus ζ plane delimiting regions with opposite direction of movement, as is depicted in Fig. 6(b) for suspended colloidal particles (note that the osmotic flow is always opposite to the movement of free particles).

It is important to address that this result could be useful for separation purposes. Given a suspension with not equally charged particles (different magnitudes and/or types, positive or negative, of charge), some of them can be selected to move in a desired direction while all the others move in the opposite, if we properly tune the gradient of electrolyte concentration and the electric current. Furthermore, even though the motion against the gradient is smaller in magnitude than if the velocity is directed toward higher concentration, it is worth to realize that the former case, the particle will be accelerated as it moves toward lower concentration (the decrease in c_0 increases the local field for a given current). On the contrary, the opposite will happen to a particle moving in the direction of higher concentration, which will undergo

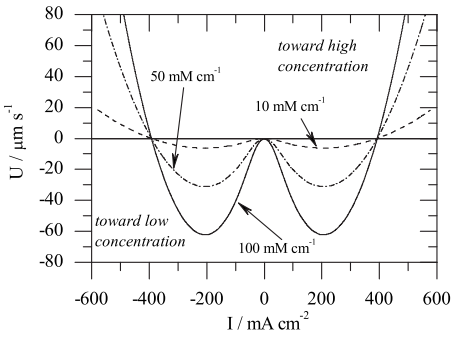

FIG. 7. Induced-charge EDV of an ideally polarizable, spherical colloidal particle as a function of the applied density current for the indicated values of the electrolyte concentration gradient. Other parameters are: $a=1$ μm, $c_0=1$ mM KCl, and $\beta=0$.

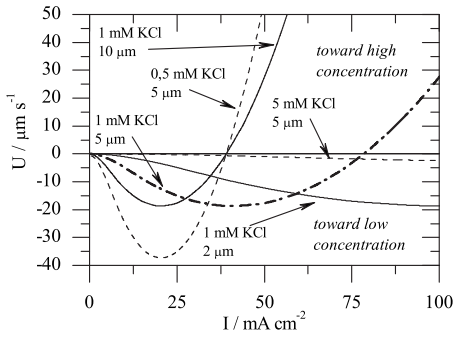

FIG. 8. Induced-charge EDV for ideally polarizable spheres, as in Fig. 7, only for different indicated values of the size of the particle and electrolyte concentration. Other parameters are: $g_\infty=30$ mM cm^{-1} and $\beta=0$.

deceleration. Consequently, we expect good efficiency in separating such colloidal particles, by taking advantage of this technique.

B. Induced-charge

For fixed charge particles, EDP is simply a nonlinear combination of classical electrophoresis and diffusiophoresis, but for polarizable particles the situation of "induced-charge EDP" is rather different and novel. We consider here situations where $\beta=0$, as its effects are of second order on $\tilde{c}_g$ and almost negligible in presence of an electric current. Before analyzing numerical results, we insist on the already mentioned $\tilde{c}_j^2$ dependence. Although it would require a much more careful study, the application of an ac field suggests interesting technological applications. As the motion does not depend on the sign of the applied current (see Fig. 7), such a field would provide net motion (whose sign would depend on the magnitude of the current), while we benefit from the advantages of an ac signal (namely, avoiding Faradaic currents at the interfaces, which degrade the structures and deliver bubbles to the bulk. Furthermore, an ac field gives no net motion in the case of fixed charge surfaces. On the other hand, note that these Faradaic reactions are able to produce net motion of bimetallic nanorods).[57,58] Roughly speaking, a finite time $\tau_c \sim \lambda_D a/D$ is needed to achieve the stationary state here described and hence an optimal frequency would exist that optimizes the effects. Typically, ac electrokinetics have an optimal performance at frequencies verifying $\omega\tau_c \sim 1$.

Let us now consider the behavior shown in Fig. 7, where the velocity is calculated numerically as a function of the electric current for different values of the gradient. In the low-$\tilde{c}_j$ and low-$\tilde{c}_g$ regime, as predicted by Eq. (59), the motion is directed toward low concentration (negative sign). As the current increases, the velocity curve describes a maximum in the direction opposite to the gradient and then the movement is reversed. For currents larger than this inversion value I_{inv}, the velocity is directed toward high electrolyte concentration, Eq. (66). Fast motions can be achieved in this regime, as the velocity increases with the square of the current. Note that $\tilde{c}_g$ only scales the magnitude of the velocity, as I_{inv} does not depend on it.

The impact of particle size and electrolyte concentration shows very interesting results, as revealed in Fig. 8. It is clear from this plot that the transition to the large-$\tilde{c}_j$ regime (motion toward higher concentrations, or positive velocities in Fig. 8) appears at lower currents the larger the size of the particle and the lower the electrolyte concentration. In this regime, large values of particle velocity, or more interestingly, of the induced flow around a fixed post, can be reached.

This result could have interesting technological applications in electrodialysis or desalination by perm-selective membranes, in a similar way as second kind electro-osmosis was previously proposed.[59] Consider a post made of an ideally polarizable material close to a perm-selective membrane in a desalination device. When the liquid has a large amount of ions in solution, the electric field drives a large current associated with these ions, which are removed from the solution through the membrane. In this situation, the flow around the post is almost zero, as the induced-charge is also very small (consider the $c_0=5$ mM KCl curve in Fig. 8). When the ionic strength of the solution is lowered via the desalination process, the conductivity is also diminished, reducing the capability of the field to remove ions by electromigration. Furthermore, strong concentration polarization is produced close to the membrane, avoiding the motion of ions out of the cavity where the solution is contained. On the other hand, in such circumstances the flow around the post is "switched on" (curve $c_0=1$ mM KCl, $a=5$ μm, or $c_0=0.5$ mM KCl in Fig. 8) and, for large enough current, it will be directed toward lower electrolyte concentration. Ions are transported from the high concentration to the low concentration side, thus reinforcing the electric current and overcoming the limiting current present in these processes. Note that this effect also occurs in the case of fixed charge surfaces due to the dependence of the electrophoretic term on c_0. This dependence increases the flow generated around structures when the concentration is lowered, but the "switching" takes place at larger values of c_0 and more gradually. In this case, the direction of the flow can be chosen by appropriately designing the device, that is, by controlling the signs of both the surface charge and the applied current.

It is worth emphasizing the c_0^{-3} dependence of the veloc-

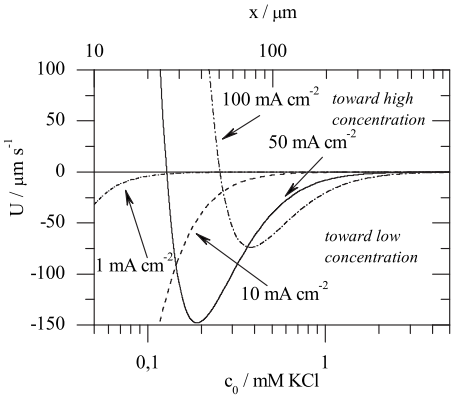

FIG. 9. EDV of an ideally polarizable sphere in a microchannel as a function of c_0, for the indicated values of the applied electric density current. The upper abscissa indicates the corresponding position, where the origin of the frame of reference verifies $c_0(x=0)=0$. Other parameters are: $g_\infty=50$ mM cm^{-1}, $a=1$ μm, and $\beta=0$.

ity, especially in the case of moderate and large values of the concentration gradient. For example, according to Eq. (65), a polarizable particle that starts moving toward high concentration (large-$\tilde{c}_j$ regime) at a position where $c_0=1$ mM KCl, subjected to a gradient $g_\infty=50$ mM KCl, would lose 70% of its velocity over a distance of 100 μm. This behavior is depicted in Fig. 9, where the velocity is plotted as a function of position along a channel and the corresponding electrolyte concentration (represented by the two abscissas). As it is seen, the velocity of a particle changes dramatically depending on its position along the channel. The magnitude of the applied current has also a crucial effect, as it determines the regime of movement, as shown in Fig. 7.

It is interesting to observe that, if the current is large enough, positions of zero velocity can exist where the particles would accumulate. Note also that these positions are stable, as any perturbation tends to move the particles toward this zero velocity position. In connection with that, highly concentrated plugs have already been observed in the experiments by Ref. 55 in the case of charged species. Although in their experiments the fluid flow plays an essential role, as theoretically analyzed by Ref. 32, the present results predict the possibility of obtaining such plugs made of polarizable particles.

Finally, we must refer at this point to the differences between the predicted flow patterns. As shown in Figs. 3–5, the effects of polarizable surfaces on the fluid flow are expected to present a richer phenomenology than those due to surfaces with fixed charge. Such flows and hydrodynamic interactions among neighboring units would be interesting topics for further study.

V. CONCLUSIONS

In this work, we have investigated the electrokinetic response to an applied direct current for a colloidal particle (electrodiffusiophoresis) or a fixed microfluidic post (electrodiffusio-osmosis) in an electrolyte solution, depending on the associated gradient of salt concentration (or transport number of the current carrying ion). Assuming thin double layers, low surface conductivity ($\mathrm{Du}\ll 1$) and negligible convective transport of ions ($\mathrm{Pe}\ll 1$), we have obtained approximate analytical expressions and full numerical solutions for the fluid flow and particle velocity for surfaces of either constant-charge or constant potential (ideally polarizable). In the case of fixed charge surfaces, movement toward high or low electrolyte concentration can be obtained by appropriately tuning the parameters, and even opposite motion for the same type of charge (positive or negative) can be achieved. Ideally polarizable surfaces show an even richer phenomenology. The direction of motion does not depend on the sign of the current, only on its magnitude, and two regimes of motion are predicted for small and large applied currents. The strong dependence found for the velocities on both size and electrolyte concentration suggests interesting new possibilities for technological applications, e.g., to mixing by posts near membranes approaching a limiting current or to new kinds of colloidal separations in electrochemical cells.

ACKNOWLEDGMENTS

Financial support from the Spanish Ministry of Education (for a FPU grant to R.A.R.) and the National Science Foundation under Contract No. DMS-0707641 (M.Z.B.) is gratefully acknowledged.

[1] J. Lyklema, *Fundamentals of Interface and Colloid Science* (Academic, San Diego, CA, 1995), Vol. II.
[2] S. S. Dukhin, "Electrokinetic phenomena of the second kind and their applications," Adv. Colloid Interface Sci. **35**, 173 (1991).
[3] V. A. Murtsovkin, "Nonlinear flows near polarized disperse particles," Colloid J. **58**, 341 (1996).
[4] A. Ramos, H. Morgan, N. G. Green, and A. Castellanos, "Ac electric-field-induced fluid flow in microelectrodes," J. Colloid Interface Sci. **217**, 420 (1999).
[5] T. M. Squires and M. Z. Bazant, "Induced-charge electro-osmosis," J. Fluid Mech. **509**, 217 (2004).
[6] M. Z. Bazant and T. M. Squires, "Induced-charge electrokinetic phenomena," Curr. Opin. Colloid Interface Sci. **15**, 203 (2010).
[7] A. Ajdari, "Pumping liquids using asymmetric electrode arrays," Phys. Rev. E **61**, R45 (2000).
[8] M. Z. Bazant and T. M. Squires, "Induced-charge electrokinetic phenomena: Theory and microfluidic applications," Phys. Rev. Lett. **92**, 066101 (2004).
[9] N. Loucaides, A. Ramos, and G. E. Georghiou, "Novel systems for configurable ac electroosmotic pumping," Microfluid. Nanofluid. **3**, 709 (2007).
[10] C. C. Huang, M. Z. Bazant, and T. Thorsen, "Ultrafast high-pressure ac electro-osmotic pumps for portable biomedical microfluidics," Lab Chip **10**, 80 (2010).
[11] T. M. Squires and M. Z. Bazant, "Breaking symmetries in induced-charge electro-osmosis and electrophoresis," J. Fluid Mech. **560**, 65 (2006).
[12] S. Gangwal, O. J. Cayre, M. Z. Bazant, and O. D. Velev, "Induced-charge electrophoresis of metallodielectric particles," Phys. Rev. Lett. **100**, 058302 (2008).
[13] J. A. Levitan, S. Devasenathipathy, V. Studer, Y. Ben, T. Thorsen, T. M. Squires, and M. Z. Bazant, "Experimental observation of induced-charge electro-osmosis around a metal wire in a microchannel," Colloids Surf., A **267**, 122 (2005).
[14] A. J. Pascall and T. M. Squires, "Induced charge electroosmosis over controllably-contaminated electrodes," Phys. Rev. Lett. **104**, 088301 (2010).
[15] M. Z. Bazant, M. S. Kilic, B. D. Storey, and A. Ajdari, "Towards an understanding of induced-charge electrokinetics at large applied voltages in concentrated solutions," Adv. Colloid Interface Sci. **152**, 48 (2009).

[16]B. V. Deryaguin, S. S. Dukhin, and A. A. Korotkova, "Diffusiophoresis in electrolyte solutions and its role in mechanism of film formation from rubber latexes by method of ionic deposition," Kolloidn. Zh. **23**, 53 (1961).
[17]S. S. Dukhin and B. V. Derjaguin, *Surface and Colloid Science* (Wiley, New York, 1974), Vol. 7.
[18]D. C. Prieve, J. L. Anderson, J. P. Ebel, and M. E. Lowell, "Motion of a particle generated by chemical gradients. Part 2. Electrolytes," J. Fluid Mech. **148**, 247 (1984).
[19]J. L. Anderson, "Colloid transport by interfacial forces," Annu. Rev. Fluid Mech. **21**, 61 (1989).
[20]H. J. Keh and L. Y. Hsu, "Diffusioosmotic flow of electrolyte solutions in fibrous porous media at arbitrary zeta potential and double-layer thickness," Microfluid. Nanofluid. **7**, 773 (2009).
[21]B. Abécassis, C. Cottin-Bizonne, C. Ybert, A. Ajdari, and L. Bocquet, "Osmotic manipulation of particles for microfluidic applications," New J. Phys. **11**, 075022 (2009).
[22]J. P. Hsu, W. L. Hsu, and Z. S. Chen, "Boundary effect on diffusiophoresis: Spherical particle in a spherical cavity," Langmuir **25**, 1772 (2009).
[23]J. Lou, C. Y. Shih, and E. Lee, "Diffusiophoresis of concentrated suspensions of spherical particles with charge-regulated surface: Polarization effect with nonlinear Poisson-Boltzmann equation," Langmuir **26**, 47 (2010).
[24]E. S. Malkin and A. S. Dukhin, "Aperiodic electrodiffusiophoresis," Colloid J. **44**, 225 (1982).
[25]*Interfacial Electrokinetic and Electrophoresis*, edited by A. V. Delgado (Marcel Dekker, New York, 2002).
[26]Y. C. Chang and H. J. Keh, "Diffusiophoresis and electrophoresis of a charged sphere perpendicular to two plane walls," J. Colloid Interface Sci. **322**, 634 (2008).
[27]S. E. Yalcin, S. Y. Lee, S. W. Joo, O. Baysal, and S. Qian, "Electrodiffusiophoretic motion of a charged spherical particle in a nanopore," J. Phys. Chem. B **114**, 4082 (2010).
[28]T. M. Squires and S. R. Quake, "Microfluidics: Fluid physics at the nanoliter scale," Rev. Mod. Phys. **77**, 977 (2005).
[29]V. I. Vasil'eva, V. A. Shaposhnik, O. V. Grigorchuk, and M. D. Malykhin, "Electrodialysis kinetics by laser interferometry," Russ. J. Electrochem. **38**, 846 (2002).
[30]Y. C. Wang, A. L. Stevens, and J. Y. Han, "Million-fold preconcentration of proteins and peptides by nanofluidic filter," Anal. Chem. **77**, 4293 (2005).
[31]S. J. Kim, Y. C. Wang, J. H. Lee, H. Jang, and J. Han, "Concentration polarization and nonlinear electrokinetic flow near a nanofluidic channel," Phys. Rev. Lett. **99**, 044501 (2007).
[32]A. Plecis, C. Nanteuil, A. M. Haghiri-Gosnet, and Y. Chen, "Electropreconcentration with charge-selective nanochannels," Anal. Chem. **80**, 9542 (2008).
[33]A. Mani, T. A. Zangle, and J. G. Santiago, "On the propagation of concentration polarization from microchannel-nanochannel interfaces Part I: Analytical model and characteristic analysis," Langmuir **25**, 3898 (2009).
[34]T. A. Zangle, A. Mani, and J. G. Santiago, "On the propagation of concentration polarization from microchannel/nanochannel interfaces Part II: Numerical and experimental study," Langmuir **25**, 3909 (2009).
[35]I. Corni, M. P. Ryan, and A. R. Boccaccini, "Electrophoretic deposition: From traditional ceramics to nanotechnology," J. Eur. Ceram. Soc. **28**, 1353 (2008).
[36]A. S. Khair and T. M. Squires, "Fundamental aspects of concentration polarization arising from nonuniform electrokinetic transport," Phys. Fluids **20**, 087102 (2008).
[37]K. T. Chu and M. Z. Bazant, "Nonlinear electrochemical relaxation around conductors," Phys. Rev. E **74**, 011501 (2006).
[38]N. A. Mishchuk and S. S. Dukhin, "Electrophoresis of solid particles at large peclet numbers," Electrophoresis **23**, 2012 (2002).
[39]J. Newman, *Electrochemical Systems*, 2nd ed. (Prentice-Hall, Englewood Cliffs, NJ, 1991).
[40]S. S. Dukhin and B. V. Deryaguin, *Electrophoresis* (Nauka, Moscow, 1976), (in Russian).
[41]I. Rubinstein and B. Zaltzman, "Electro-osmotic slip of the second kind and instability in concentration polarization at electrodialysis membranes," Math. Models Meth. Appl. Sci. **11**, 263 (2001).
[42]B. Zaltzman and I. Rubinstein, "Electro-osmotic slip and electroconvective instability," J. Fluid Mech. **579**, 173 (2007).
[43]E. Yariv, "Nonlinear electrophoresis of ideally polarizable particles," Europhys. Lett. **82**, 54004 (2008).
[44]H. A. Stone and A. D. T. Samuel, "Propulsion of microorganisms by surface distortions," Phys. Rev. Lett. **77**, 4102 (1996).
[45]M. Z. Bazant, "Conformal mapping of some non-harmonic functions in transport theory," Proc. R. Soc. London, Ser. A **460**, 1433 (2004).
[46]M. Z. Bazant, K. T. Chu, and B. J. Bayly, "Current-voltage relations for electrochemical thin films," SIAM J. Appl. Math. **65**, 1463 (2005).
[47]A. Bonnefont, F. Argoul, and M. Z. Bazant, "Analysis of diffuse-layer effects on time-dependent interfacial kinetics," J. Electroanal. Chem. **500**, 52 (2001).
[48]H. J. Keh and Y. K. Wei, "Diffusiophoretic mobility of spherical particles at low potential and arbitrary double-layer thickness," Langmuir **16**, 5289 (2000).
[49]H. Ohshima, *Electrical Phenomena at Interfaces: Fundamentals, Measurements, and Applications* (CRC, New York, 1998), pp. 19–55.
[50]M. J. Lighthill, "On the squirming motion of nearly spherical deformable bodies through liquids at very small Reynolds numbers," Commun. Pure Appl. Math. **5**, 109 (1952).
[51]J. R. Blake, "A spherical envelope approach to ciliary propulsion," J. Fluid Mech. **46**, 199 (1971).
[52]G. K. Batchelor, *An Introduction to Fluid Dynamics* (Cambridge University Press, Cambridge, 1967).
[53]C. M. Bender and S. A. Orszag, *Advanced Mathematical Methods for Scientists and Engineers* (McGraw-Hill, New York, NY, 1978).
[54]S. Barany, "Electrophoresis in strong electric fields," Adv. Colloid Interface Sci. **147-148**, 36 (2009).
[55]S. J. Kim, L. D. Li, and J. Han, "Amplified electrokinetic response by concentration polarization near nanofluidic channel," Langmuir **25**, 7759 (2009).
[56]S. S. Dukhin, "Non-equilibrium electric surface phenomena," Adv. Colloid Interface Sci. **44**, 1 (1993).
[57]J. Burdick, R. Laocharoensuk, P. M. Wheat, J. D. Posner, and J. Wang, "Synthetic nanomotors in microchannel networks: Directional microchip motion and controlled manipulation of cargo," J. Am. Chem. Soc. **130**, 8164 (2008).
[58]J. L. Moran, P. M. Wheat, and J. D. Posner, "Locomotion of electrocatalytic nanomotors due to reaction induced charge autoelectrophoresis," Phys. Rev. E **81**, 065302 (2010).
[59]N. A. Mishchuk, "Perspectives of the electrodialysis intensification," Desalination **117**, 283 (1998).